



# DNA damage triggers reprogramming of differentiated cells into stem cells in *Physcomitrella*

Nan Gu<sup>1,2,3,8</sup>, Yosuke Tamada<sup>3,4,5,6,8</sup>, Akihiro Imai<sup>3</sup>, Gergo Palfalvi<sup>3,4</sup>, Yukiko Kabeya<sup>3</sup>, Shuji Shigenobu<sup>3,4</sup>, Masaki Ishikawa<sup>3,4</sup>, Karel J. Angelis<sup>7</sup>, Chunli Chen<sup>1,2</sup>✉ and Mitsuyasu Hasebe<sup>3,4</sup>✉

**DNA damage can result from intrinsic cellular processes and from exposure to stressful environments. Such DNA damage generally threatens genome integrity and cell viability<sup>1</sup>. However, here we report that the transient induction of DNA strand breaks (single-strand breaks, double-strand breaks or both) in the moss *Physcomitrella patens* can trigger the reprogramming of differentiated leaf cells into stem cells without cell death. After intact leafy shoots (gametophores) were exposed to zeocin, an inducer of DNA strand breaks, the *STEM CELL-INDUCING FACTOR 1 (STEMIN1)*<sup>2</sup> promoter was activated in some leaf cells. These cells subsequently initiated tip growth and underwent asymmetric cell divisions to form chloronema apical stem cells, which are in an earlier phase of the life cycle than leaf cells and have the ability to form new gametophores. This DNA-strand-break-induced reprogramming required the DNA damage sensor ATR kinase, but not ATM kinase, together with *STEMIN1* and closely related proteins. ATR was also indispensable for the induction of *STEMIN1* by DNA strand breaks. Our findings indicate that DNA strand breaks, which are usually considered to pose a severe threat to cells, trigger cellular reprogramming towards stem cells via the activity of ATR and *STEMIN1*s.**

Wounding is a general trigger for reprogramming differentiated plant cells into stem cells<sup>3</sup>. In angiosperms, the ablation of the shoot apical meristem or excision of the root tip induces the reprogramming of peripheral cells to establish a new stem cell niche<sup>4,5</sup>. This process requires factors including the phytohormone auxin and the AP2/ERF transcription factor ERF115 (refs. 6–8). Stem cell death (for example, due to DNA damage) similarly serves as a signal that induces the reprogramming of peripheral cells towards the stem cell niche<sup>6,9,10</sup>. In addition, explants cultured with phytohormones can form a mass of undifferentiated cells known as a callus at the excision site. When this callus is further cultured with the appropriate concentrations of phytohormones, shoot or root apical meristems containing stem cells are regenerated<sup>11,12</sup>.

In the moss *Physcomitrella patens* (*Physcomitrella*), leaf excision causes differentiated leaf cells next to the excision site (edge cells) to be reprogrammed into chloronema apical stem cells within 48 h

of culture without phytohormones (Fig. 1a,b and Extended Data Fig. 1a)<sup>13–15</sup>. Chloronema apical stem cells are the first cell type formed from germinating *Physcomitrella* spores and thus represent an earlier phase of the life cycle compared with leaf cells. Like other chloronema apical stem cells, the wound-induced stem cells generated new leafy shoots known as gametophores, which continuously produced new leaves (Extended Data Fig. 2)<sup>16</sup>.

To analyse the role of DNA strand breaks (single-strand breaks (SSBs), double-strand breaks (DSBs) or both) in the reprogramming, we incubated excised *Physcomitrella* leaves with the DNA-strand-break inducers zeocin<sup>17</sup>, bleomycin (BLM)<sup>18</sup> and camptothecin (CPT)<sup>19</sup> at concentrations in which cell divisions of protonemata (hypha-like structures including chloronema cells) were attenuated but did not stop (Extended Data Fig. 1b–d). Unexpectedly, the percentage of excised leaves with reprogrammed non-edge cells increased from ~25% to 60% (Fig. 1a–c). These results suggest that reagents that initiate DNA strand breaks enhance the reprogramming of excised leaf cells.

To determine whether leaf cell reprogramming could be induced by DNA strand breaks without wounding, we exposed intact gametophores to DNA-strand-break-inducing reagents. No stem cells formed in response to the same concentrations used in excised leaves (Fig. 1d,e). However, when intact gametophores were transiently immersed in 50 µg ml<sup>-1</sup> zeocin, 20 µg ml<sup>-1</sup> BLM or 30 µM CPT for 6 h and cultivated for 7 d without reagents, leaf cells were reprogrammed to form chloronema apical stem cells in approximately 70% of intact gametophores (Fig. 1f,g). Two weeks after the removal of zeocin or BLM, new gametophores formed from the protonemata (Extended Data Fig. 2k), indicating that protonema apical stem cells formed from leaf cells in response to DNA-strand-break-inducing reagents had the developmental ability to produce gametophores.

To quantify DNA strand breaks in gametophores after transient exposure to zeocin, BLM or CPT, we performed a neutral (N/N) comet assay, which is commonly used to identify DSBs<sup>20,21</sup>. BLM induced approximately 90% DSB formation, whereas a significant increase of damaged DNA induced by zeocin or CPT with the N/N comet assay was not detected (Fig. 2a,b). An alkaline (A/A) comet assay to detect DSBs and SSBs<sup>20,21</sup> revealed that BLM induced the

<sup>1</sup>College of Life Science and Technology, Huazhong Agricultural University, Wuhan, P.R. China. <sup>2</sup>Key Laboratory of Horticultural Plant Biology (Ministry of Education), Huazhong Agricultural University, Wuhan, P.R. China. <sup>3</sup>Division of Evolutionary Biology, National Institute for Basic Biology, Okazaki, Japan. <sup>4</sup>Department of Basic Biology, The Graduate University for Advanced Studies, SOKENDAI, Okazaki, Japan. <sup>5</sup>School of Engineering, Utsunomiya University, Utsunomiya, Japan. <sup>6</sup>Center for Optical Research and Education (CORE), Utsunomiya University, Utsunomiya, Japan. <sup>7</sup>Institute of Experimental Botany, Academy of Sciences of the Czech Republic, Prague, Czech Republic. <sup>8</sup>These authors contributed equally: Nan Gu, Yosuke Tamada. ✉e-mail: [chenchunli@mail.hzau.edu.cn](mailto:chenchunli@mail.hzau.edu.cn); [mhasebe@nibb.ac.jp](mailto:mhasebe@nibb.ac.jp)

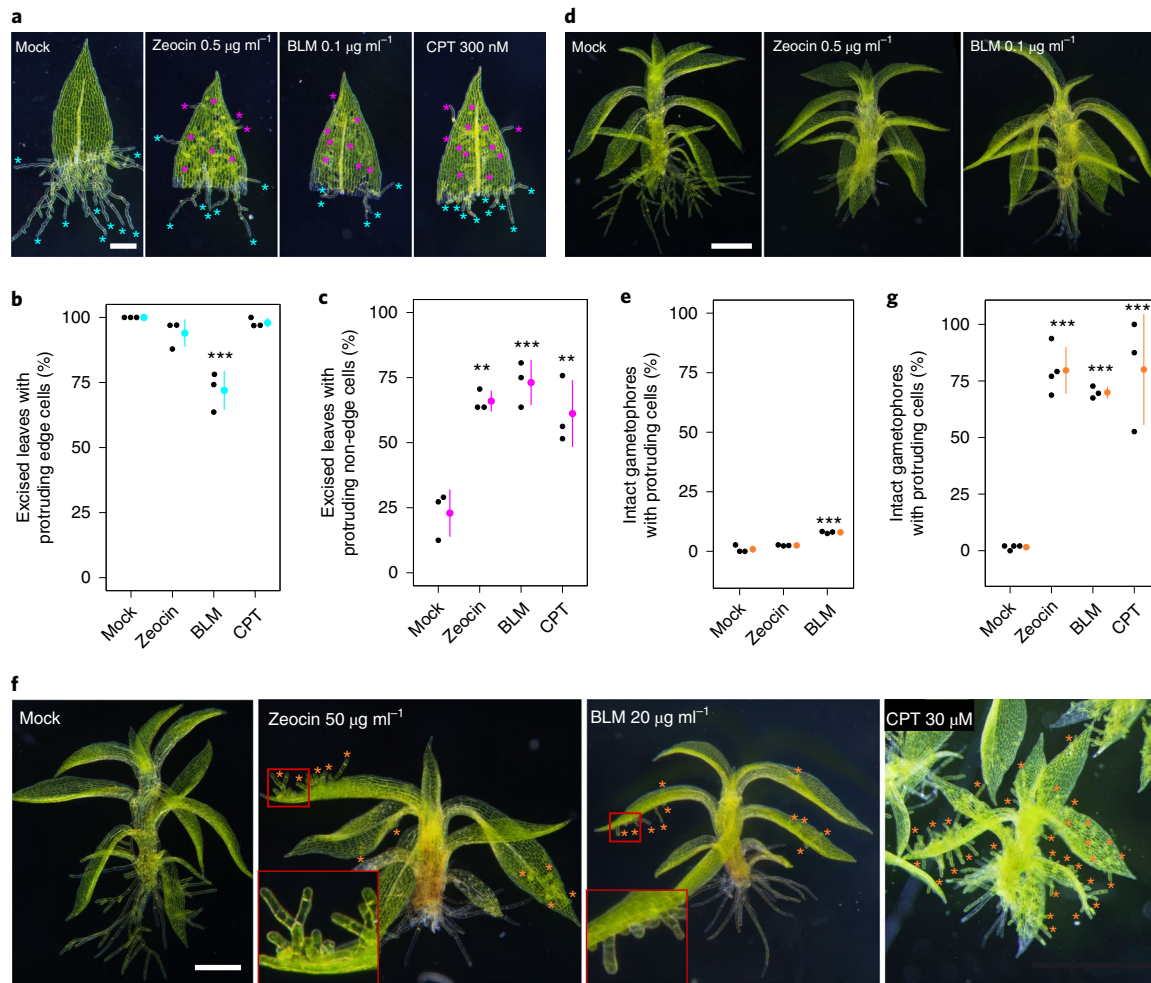


**Fig. 1 | DNA-strand-break-inducing reagents trigger the reprogramming of differentiated leaf cells into stem cells.** **a–c**, Representative excised leaves immersed in a medium with or without 0.5  $\mu\text{g ml}^{-1}$  zeocin, 0.1  $\mu\text{g ml}^{-1}$  BLM or 300 nM CPT for 3 d (**a**). The blue and violet asterisks indicate chloronema apical stem cells generated from edge and non-edge cells, respectively. The percentages of excised leaves with protruding edge (**b**) and non-edge (**c**) cells are shown. The blue and violet dots and bars represent the average and s.d. from biological triplicates ( $30 \leq n \leq 40$ , excised leaves), respectively. **d,e**, Representative gametophores continuously cultured in a medium with or without 0.5  $\mu\text{g ml}^{-1}$  zeocin or 0.1  $\mu\text{g ml}^{-1}$  BLM for 7 d (**d**), and the percentages of intact gametophores with at least one cell acquiring tip growth (**e**). The orange dots and bars represent the average and s.d., respectively, from three biological replicates ( $30 \leq n \leq 40$ , gametophores). **f,g**, Representative gametophores incubated with or without 50  $\mu\text{g ml}^{-1}$  zeocin, 20  $\mu\text{g ml}^{-1}$  BLM or 30  $\mu\text{M}$  CPT for 6 h and cultured without DNA-break-inducing reagents for an additional 7 d (**f**), and the percentages of intact gametophores with at least one cell acquiring tip growth (**g**). The orange asterisks indicate the positions of chloronema apical stem cells generated from gametophore leaves. The orange dots and bars represent the average and s.d., respectively, from four biological replicates ( $8 \leq n \leq 48$ , gametophores). \*\* $P < 0.01$ ; \*\*\* $P < 0.001$  by two-sided post hoc pairwise Dunnett tests with multiple comparisons.  $P = 4.8 \times 10^{-5}$  for BLM in **b**;  $P = 0.000116$  for zeocin,  $P = 0.00041$  for BLM and  $P = 0.00251$  for CPT in **c**;  $P = 0.00017$  for BLM in **e**;  $P = 3.6 \times 10^{-5}$  for zeocin,  $P = 6.8 \times 10^{-5}$  for BLM and  $P = 2.0 \times 10^{-5}$  for CPT in **g**. WT, wild type. Scale bars, 200  $\mu\text{m}$  in **a** and 1 mm in **d,f**.

formation of SSBs in addition to DSBs, although the SSB levels could not be quantified because the heads of the comets were nearly invisible (Fig. 2a). By contrast, we detected DNA damage induced by zeocin or CPT with the A/A assay but not the N/N assay, indicating that zeocin and CPT predominantly induce SSBs in *Physcomitrella* (Fig. 2a,b). Zeocin, BLM and CPT induce DNA strand breaks<sup>17–19</sup> in common. These results suggest that DNA strand breaks induce the reprogramming. As CPT has an obvious side effect, the inhibition of the TOP1 function, along with the SSB induction<sup>19</sup>, and zeocin seems to induce reprogramming by producing more moderate DNA strand breaks than BLM, we chose zeocin for further analysis.

Since zeocin treatment reactivated the cell cycle in leaf cells, we reasoned that the damaged DNA had been repaired. To test this notion, we measured SSB levels during and after zeocin treatment using an A/A comet assay (Fig. 2c). SSBs accumulated during and

1 h after zeocin treatment, followed by a gradual decrease. SSBs were repaired to the initial level at 30 h after the removal of zeocin (Fig. 2c). This process occurred 1 to 2 d earlier than the protrusion of leaf cells, a morphological marker of reprogramming to chloronema stem cells (Extended Data Fig. 3), suggesting that the SSBs had been repaired before cell cycle re-entry in most leaf cells.

We noticed that a few cells in gametophore leaves died in response to transient zeocin treatment (Extended Data Fig. 4a,b), which may have served as a wounding signal to induce reprogramming<sup>6,9,10</sup>. We therefore examined the viability of leaf cells peripheral to protruding cells in intact gametophores after zeocin treatment using the fluorescent dyes fluorescein diacetate (FDA) and propidium iodide (PI). FDA stains the cytosol of living cells, whereas PI penetrates into dead cells<sup>22</sup>. We examined 50 protruding chloronema apical stem cells from independent leaves, finding that only 3 stem cells were present

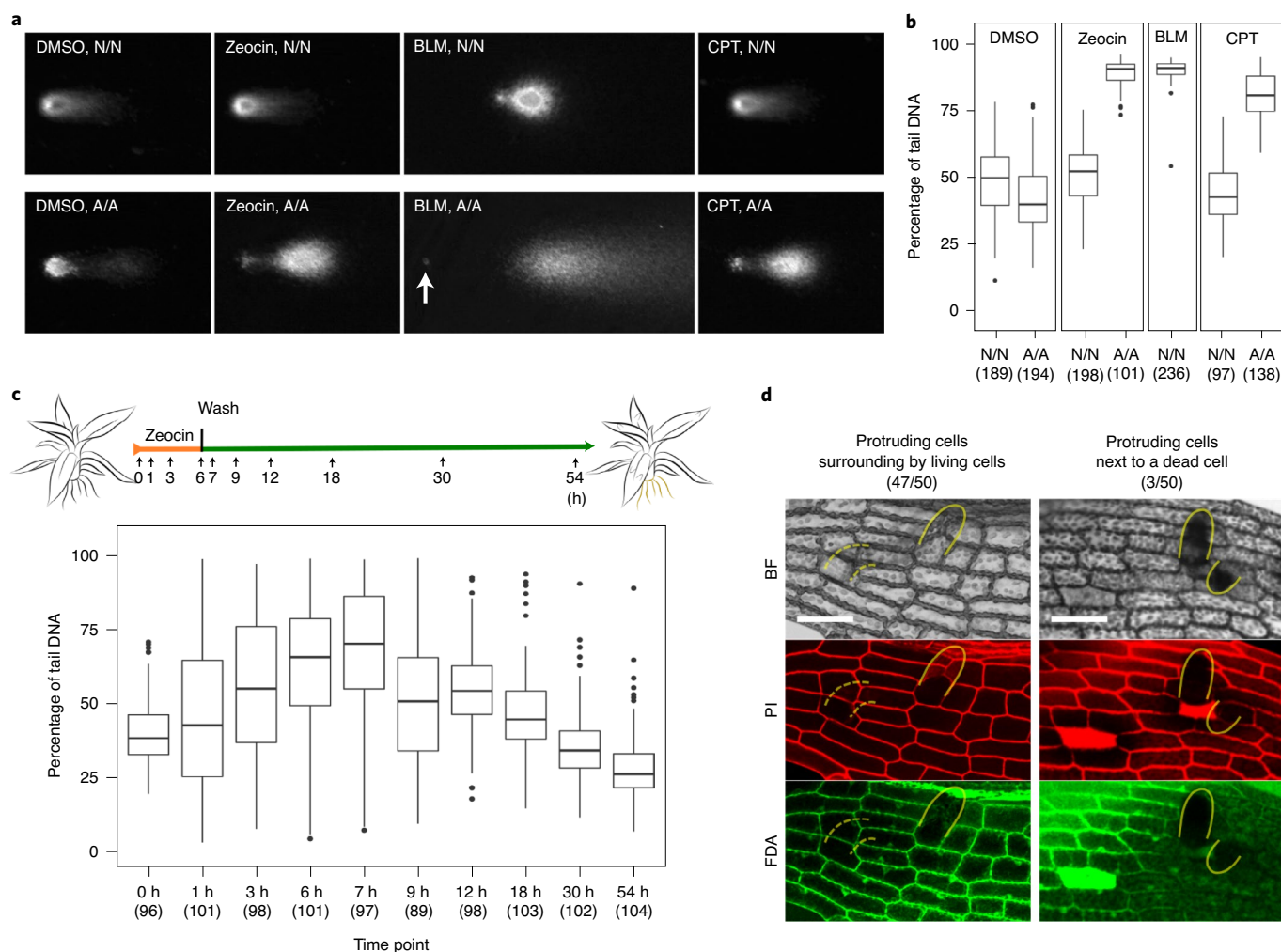


**Fig. 2 | Zeocin, BLM or CPT induces DNA strand breaks and triggers reprogramming without cell death. a**, Representative images of nuclei obtained in comet assays under N/N (top panels) and A/A (bottom panels) conditions. The nuclei were isolated from gametophores immersed in a medium with or without  $50 \mu\text{g ml}^{-1}$  zeocin,  $10 \mu\text{g ml}^{-1}$  BLM or  $30 \mu\text{M}$  CPT for 1 h. The direction of electrophoresis is left to right. The white arrow indicates the head of the nucleus. **b**, Percentages of damaged DNA in comet tails under each condition. The number of biologically independent comets examined in each condition is shown in brackets. **c**, Diagram illustrating the sampling time points during and after 6 h of treatment with  $50 \mu\text{g ml}^{-1}$  zeocin (top), and percentages of damaged DNA under A/A conditions (bottom). The number of biologically independent comets in each time point is shown in brackets. The upper and lower bounds of the boxes in **b, c** correspond to the 25th and 75th percentiles. The centre line indicates the median. The whiskers go down to the smallest value within 1.5 times the interquartile range (IQR) below the 25th percentile and up to the largest value within 1.5 times the IQR above the 75th percentile. The data beyond the ends of the whiskers are plotted individually<sup>38</sup>. The experiments were performed twice independently, with similar results. **d**, Representative leaf cells with protruding stem cells after cultivation for 6 h in  $50 \mu\text{g ml}^{-1}$  zeocin, followed by 7 d without zeocin. Cell viability was visualized by FDA and PI staining. Dead leaf cells are not collapsed and can be visible 7 d after their death. This experiment was repeated twice, with similar results. BF, bright field. Scale bars,  $50 \mu\text{m}$ .

next to dead cells, whereas the 47 remaining cells had protruded from leaves lacking dead cells (Fig. 2d). We further observed the reprogramming process every two hours with PI staining during and after the zeocin treatment. We confirmed that the reprogramming cells were observed in six gametophores with no dead cells, as leaf cells showed the active movement of chloroplasts and no PI staining inside the cells throughout the time-lapse observation (Extended Data Fig. 4c and Supplementary Video 1). Even when dead cells without chloroplast movement and with PI staining of the nuclei were observed in two gametophores, the protruding cells were not peripheral to the dead cells (Extended Data Fig. 4d and Supplementary Video 2). These results indicate that DNA-strand-break-induced reprogramming can occur in the absence of dead cells.

Cold-shock Domain Protein 1 (CSP1), a homologue of mammalian induced pluripotent stem cell factor Lin28 (ref. <sup>23</sup>) and a

stem cell marker in *Physcomitrella*, accumulates in the edge cells of excised leaves and enhances wounding-induced reprogramming<sup>15</sup>. In addition, the ectopic expression of the wounding-inducible AP2/ERF transcription factor *STEMIN1* induces reprogramming without wounding<sup>3</sup>. The disruption of *STEMINs* or *CSPs* leads to delayed reprogramming after leaf excision<sup>2,15</sup>. The cell cycle regulator *CYCD;1*, a direct target of *STEMIN1* (ref. <sup>2</sup>), is also induced after wounding, representing the re-entry of the cell cycle<sup>13</sup>. After transient zeocin treatment, *STEMIN1* and *CSP1*, as well as *CYCD;1*, were induced in some leaf cells, which eventually acquired tip growth to become chloronema stem cells (Extended Data Fig. 5 and Supplementary Videos 3–5). *STEMIN2* and *STEMIN3* were induced in all examined leaf cells after zeocin treatment at a level that was approximately one-tenth of the induction level of *STEMIN1* (Extended Data Fig. 5 and Supplementary Videos 6 and 7). To investigate

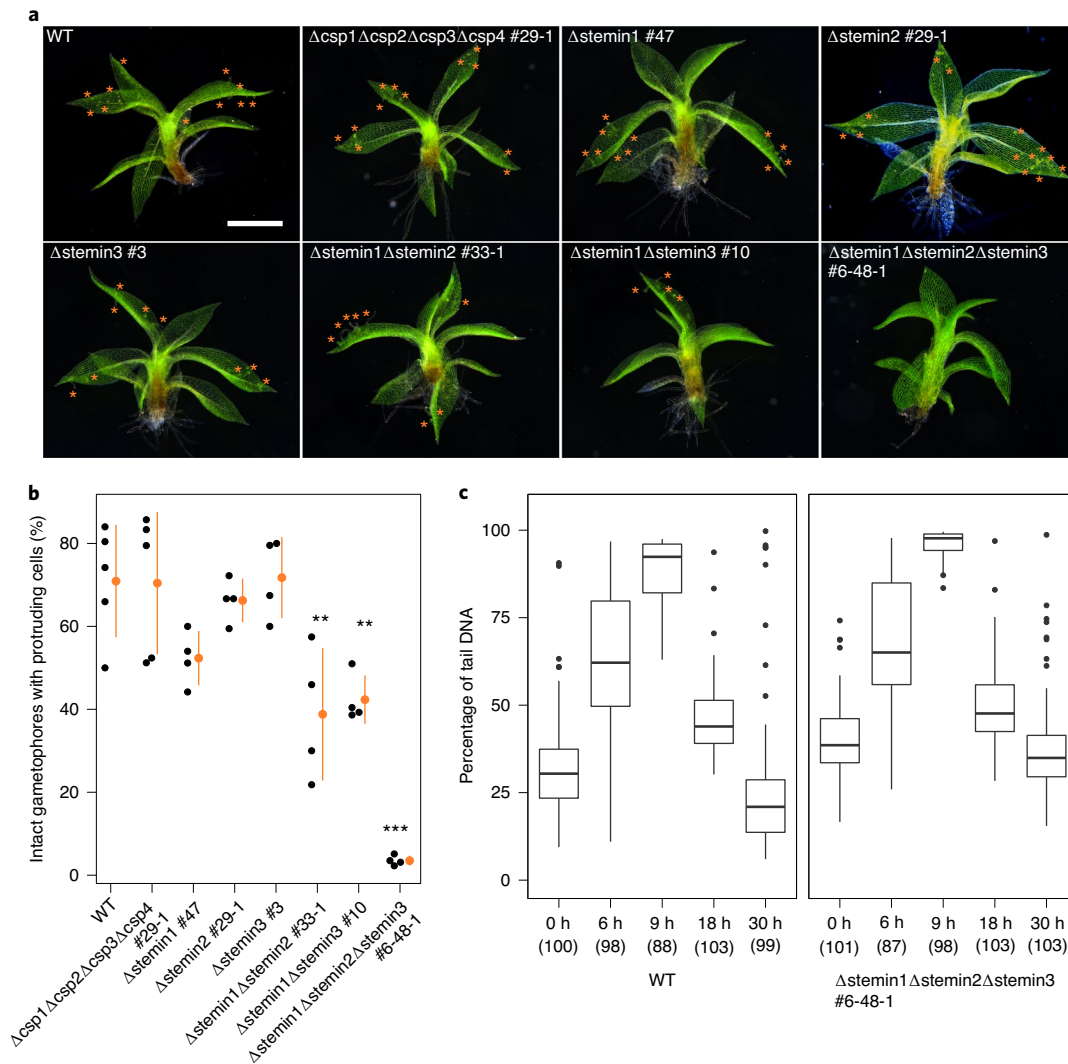


**Fig. 3 | Reprogramming induced by DNA strand breaks requires STEMINs, which function in wounding-induced reprogramming. a**, Representative WT,  $\Delta csp1\Delta csp2\Delta csp3\Delta csp4$  #29-1,  $\Delta stemin1$  #47,  $\Delta stemin2$  #29-1,  $\Delta stemin3$  #3,  $\Delta stemin1\Delta stemin2$  #33-1,  $\Delta stemin1\Delta stemin3$  #10 and  $\Delta stemin1\Delta stemin2\Delta stemin3$  #6-48-1 gametophores cultured for 7 d after 6 h of treatment with  $50\ \mu\text{g ml}^{-1}$  zeocin. The orange asterisks indicate the positions of chloronema apical stem cells generated from gametophore leaves. **b**, Percentages of intact gametophores with at least one cell acquiring tip growth. The orange dots and bars represent the average and s.d. from at least four independent experiments ( $30 \leq n \leq 55$ , gametophores), respectively.  $**P < 0.01$ ;  $***P < 0.001$  by two-sided post hoc pairwise Dunnett tests with multiple comparisons.  $P = 0.0014$  for  $\Delta stemin1\Delta stemin2$  #33-1,  $P = 0.0050$  for  $\Delta stemin1\Delta stemin3$  #10 and  $P = 4.4 \times 10^{-5}$  for  $\Delta stemin1\Delta stemin2\Delta stemin3$  #6-48-1. **c**, Percentages of damaged DNA (tail DNA) during and after zeocin treatment analysed by comet assay under A/A conditions. The number of comets analysed at each time point of each line is shown in brackets. The upper and lower bounds of the boxes correspond to the 25th and 75th percentiles. The centre line indicates the median. The whiskers go down to the smallest value within 1.5 times the IQR below the 25th percentile and up to the largest value within 1.5 times the IQR above the 75th percentile. The data beyond the ends of the whiskers are plotted individually<sup>38</sup>. The experiments were performed twice independently, with similar results. Scale bar, 1 mm.

the similarities and differences between wounding-induced and DNA-strand-break-induced reprogramming, we examined whether CSP1 and STEMIN1 are required for DNA-strand-break-induced reprogramming. Intact gametophores of a quadruple-deletion mutant of CSPs ( $\Delta csp1\Delta csp2\Delta csp3\Delta csp4$  #29-1)<sup>15</sup> and a triple-deletion mutant of STEMINs<sup>2</sup> ( $\Delta stemin1\Delta stemin2\Delta stemin3$  #6-48-1) were exposed to  $50\ \mu\text{g ml}^{-1}$  zeocin for 6 h. After 7 d of cultivation without zeocin, the CSP quadruple-deletion mutant line formed protruded stem cells from intact gametophore leaves, like the wild type (Fig. 3a,b). By contrast, protruded cells were not observed in the triple-deletion STEMIN mutant (Fig. 3a,b), indicating that DNA-strand-break-induced reprogramming requires STEMINs but not CSPs. The percentage of gametophores with

reprogrammed leaf cells was reduced by approximately 20% in a STEMIN1 single-deletion mutant ( $\Delta stemin1$  #47) and by an additional 10% in double-deletion mutants ( $\Delta stemin1\Delta stemin2$  #29-1 and  $\Delta stemin1\Delta stemin3$  #10) (Fig. 3a,b). These results indicate that STEMIN genes are redundantly required for the reprogramming induced by DNA strand breaks. In addition, SSBs induced by zeocin were repaired in the STEMIN triple-deletion mutant as in the wild type (Fig. 3c), indicating that STEMINs are not involved in SSB repair pathways; instead, they seem to play a role in reprogramming downstream of SSB repair pathways.

To examine the transcriptional responses of primary signal transducers of DNA strand breaks, including Ataxia Telangiectasia Mutated (ATM) and ATM and RAD3-related

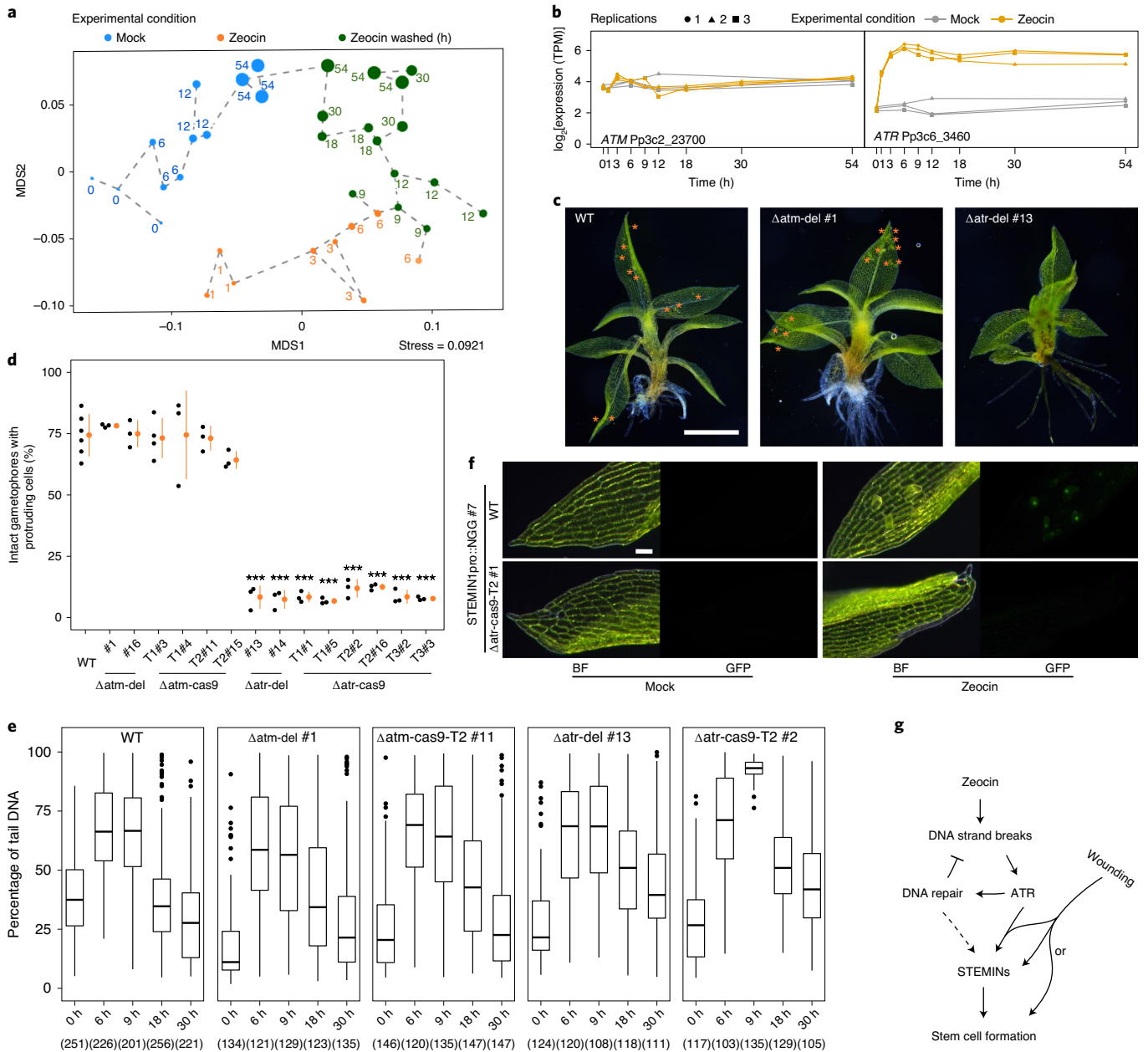


**Fig. 4 | DNA-strand-break-induced reprogramming requires the DNA damage sensor gene *ATR*.** **a**, Multidimensional scaling (MDS) plot of the transcriptome data from intact gametophores treated with  $50 \mu g ml^{-1}$  zeocin for 6 h (orange dots) and washed (green dots) or without zeocin treatment (blue dots). **b**, *ATM* and *ATR* transcript levels with (orange lines) or without zeocin treatment (grey lines). The results from three biological replicates are shown. **c**, Representative WT,  $\Delta atm$ -del #1 and  $\Delta atr$ -del #13 gametophores cultured for 7 d after 6 h of treatment with  $50 \mu g ml^{-1}$  zeocin. The orange asterisks indicate the positions of chloronema apical stem cells generated from gametophore leaves. **d**, Percentages of gametophores in which at least one cell acquired tip growth. The orange dots and bars represent the average and s.d. from at least three biological replicates ( $30 \leq n \leq 48$ , gametophores), respectively. \*\*\* $P < 0.001$  by two-sided post hoc pairwise Dunnett tests with multiple comparisons.  $P = 3.3 \times 10^{-16}$  for line  $\Delta atr$ -cas9-T2 #2, and  $P < 2.0 \times 10^{-16}$  for the other  $\Delta atr$  lines. **e**, Percentages of damaged DNA during and after zeocin treatment analysed by comet assay under A/A conditions. The number of comets at each time point of each line is shown in brackets. The upper and lower bounds of the boxes correspond to the 25th and 75th percentiles. The centre line indicates the median. The whiskers go down to the smallest value within 1.5 times the IQR below the 25th percentile and up to the largest value within 1.5 times the IQR above the 75th percentile. The data beyond the ends of the whiskers are plotted individually<sup>38</sup>. **f**, Promoter activity of *STEMIN1* after transient zeocin treatment detected in *STEMIN1*pro::NGG lines in the WT and  $\Delta atr$  backgrounds. The intact gametophores were treated with  $50 \mu g ml^{-1}$  zeocin for 6 h and cultured without zeocin for an additional 4 d. This observation was repeated twice with similar results. **g**, Model of the reprogramming induced by DNA strand breaks. TPM, transcripts per million. Scale bars, 1 mm in **c** and 100  $\mu m$  in **f**.

(*ATR*)<sup>1</sup>, and other factors related to the DNA damage response during DNA-strand-break-induced reprogramming, we performed RNA-sequencing (RNA-seq) analysis of gametophores during and after transient zeocin treatment (Supplementary Fig. 1)

at the same intervals as the DNA repair measurements (Fig. 2c). Multidimensional scaling indicated that the transcriptome markedly changed within 3 h of zeocin treatment and continued to change during 6 h of zeocin treatment (Fig. 4a). After zeocin was

removed, the direction of the trajectory of overall transcriptome profiles changed towards an increasing similarity to the mock treatment (Fig. 4a). This implies a gradual restraint of the zeocin effect and the progression of DNA repair (Fig. 2c). However, differences between the transcriptome profiles still existed between samples 54h after the treatment of mock and zeocin (Fig. 4a and Supplementary Fig. 2), reflecting the differences in transcript levels of genes related to the DNA damage response (Supplementary Fig. 1). As one such gene, *ATR* strongly increased its transcript levels during zeocin treatment and remained high even at 48h after treatment; by contrast, *ATM* transcript levels remained largely unchanged by zeocin treatment (Fig. 4b). Although the expression of *STEMIN1*, *CSP1* and *CYCD;1* increased in reprogramming cells in the time-lapse imaging analysis (Extended Data Fig. 5), we could not detect increased transcript levels of *STEMIN1*, *CSP1*, *CYCD;1* and other genes involved in wounding-induced reprogramming (Supplementary Fig. 3), probably because only a limited number of cells were reprogrammed.

To determine whether DNA-strand-break-induced reprogramming requires the sensor kinases ATM and ATR, we generated  $\Delta atm$  and  $\Delta atr$  deletion mutants (Supplementary Figs. 4 and 5). Protonemata and gametophores of the  $\Delta atm$  deletion mutant lines were indistinguishable from those of the wild type, whereas the  $\Delta atr$  deletion mutant lines had smaller gametophores with shorter leaves than the wild type (Fig. 4c and Supplementary Fig. 6). These changes were probably caused by defects in cell division, since ATR evokes DNA damage responses by sensing replication stress during development<sup>24</sup>. Both  $\Delta atm$  and  $\Delta atr$  mutants retained the ability to undergo reprogramming induced by wounding, like the wild type (Extended Data Fig. 6). The  $\Delta atm$  mutants also exhibited DNA-strand-break-induced reprogramming, like the wild type (Fig. 4c,d). By contrast, the frequency of DNA-strand-break-induced reprogramming was sharply reduced in the  $\Delta atr$  mutants (Fig. 4c,d). These results suggest that ATR, but not ATM, functions in the pathway from DNA damage sensing to reprogramming. The SSB repair process of the  $\Delta atm$  mutants was similar to that of the wild type in the A/A comet assay (Fig. 4e). By contrast, the SSB repair process of the  $\Delta atr$  mutants was delayed compared with that of the wild type but was not completely blocked (Fig. 4e). The transcript levels of nine representative DNA damage response genes were less increased in both  $\Delta atm$  and  $\Delta atr$  mutants compared with those in the wild type after transient zeocin treatment (Extended Data Fig. 7). These findings indicate that both ATM and ATR function in activating DNA damage response genes for the repair of DNA strand breaks induced by zeocin, and they suggest that SSB repair in the absence of ATR is not sufficient to induce reprogramming or that ATR activity is involved in the reprogramming process.

In a line containing the *STEMIN1* promoter fused with GFP harbouring wild-type *ATR* (*STEMIN1*pro::NGG [NLS-sGFP-GUS])<sup>2</sup>, GFP signals were detected in some leaf cells beginning approximately 44h after transient zeocin treatment and continuously accumulated until the initiation of tip growth approximately 64h after zeocin treatment (Fig. 4f [top panels], Extended Data Fig. 5 and Supplementary Video 5). To analyse the role of *ATR* in the induction of *STEMIN1*, we generated  $\Delta atr$  knockout mutant lines using the CRISPR-Cas9 system<sup>25</sup> in the *STEMIN1*pro::NGG background (Supplementary Fig. 7). In the absence of *ATR*, no leaf cells with GFP expression driven by the *STEMIN1* promoter were detected after transient zeocin treatment (Fig. 4f, bottom panels). These results indicate that the induction of *STEMIN1* by DNA strand breaks depends on ATR. Together, our data reveal that transient and repairable DNA strand breaks are a trigger of cellular reprogramming, which requires STEMINs and ATR (Fig. 4g).

In summary, STEMINs function in both wounding-induced and DNA-damage-induced reprogramming. By contrast, ATR functions in DNA-damage-induced but not wounding-induced reprogramming.

Moreover, the period required for DNA-damage-induced reprogramming (approximately 60h) is longer than that required for wounding-induced reprogramming (approximately 30h). Taken together, it seems that the wounding-induced and DNA-damage-induced reprogramming pathways are different, but converge at or upstream of STEMINs. It is a future challenge to explore the mechanisms of how DNA damage response connects to STEMIN induction, and analyses of transcriptome changes in  $\Delta atr$  mutants will be informative. In the natural environment, DNA strand breaks are repeatedly induced under chilling conditions, the existence of heavy metals or oxidative stresses (including ultraviolet radiation)<sup>26–28</sup>. Unlike most animals, sessile *Physcomitrella* may utilize reprogramming after substantial but repairable DNA strand breaks to form fast-growing protonema cells to escape from a local area with genotoxic stress before it accumulates in the genome. It will be interesting to investigate whether DNA strand breaks play a positive role in reprogramming in other organisms and whether natural stresses induce reprogramming in the absence of wounding. Repairable DNA strand breaks can induce genome-wide changes in the chromatin landscape to initiate DNA repair<sup>29,30</sup>. This process may compromise the fate of differentiated cells and induce competency towards reprogramming. Another possibility is that some signals are released from alive but damaged cells to less-damaged neighbouring cells to trigger the reprogramming. Our study provides a viewpoint for exploring the relationship between DNA strand breaks and cellular reprogramming from differentiated cells to stem cells without cell death.

## Methods

**Plant materials and growth conditions.** *Physcomitrella patens* Gransden 2004 strain<sup>31</sup> was used as the wild type. The *Physcomitrella* was grown on solid BCDAT medium at 25°C under continuous white light for protonema propagation<sup>32</sup>. To efficiently collect the protonemata, a layer of cellophane was placed onto the medium<sup>33</sup>. To induce gametophore formation, the protonemata were propagated on solid BCDAT medium without cellophane and cultured at 25°C under continuous white light for three to four weeks. To induce reprogramming caused by wounding, the third to fifth visible leaves from the apex of each gametophore were excised (by cutting) and cultivated in liquid BCDAT medium<sup>31</sup>. To induce DNA strand breaks, the excised leaves or intact gametophores were placed into liquid BCDAT medium with or without zeocin (Invitrogen, CAS11006-33-0), BLM (LKT, CAS9041-93-4) or CPT (Sigma, CAS7689-03-4). To transiently induce DNA strand breaks, the intact gametophores were treated with zeocin, BLM or CPT for 6h, washed and transferred into liquid BCDAT medium without DNA-strand-break-inducing reagents.

**Analysis of cell death via fluorescence imaging.** Cell death was analysed as previously described<sup>22</sup> with some modifications. The gametophores were submerged in 4ml of BCDAT liquid medium with 10  $\mu$ l of 1 mg ml<sup>-1</sup> PI (Wako, 25535-16-4) and cultured for 3h in the dark. The gametophores were stained by adding 2  $\mu$ l of 10 mg ml<sup>-1</sup> FDA (Sigma, CAS596-09-8) dissolved in acetone to the medium, followed by 1h of incubation in the dark. The samples were observed under a confocal microscope with a  $\times 10$  objective lens and a white-light laser (SP8, Leica). PI fluorescence was detected at 580–650 nm under an excitation wavelength of 540 nm. FDA fluorescence was detected at 510–529 nm under an excitation wavelength of 488 nm. For the time-lapse observations, the gametophores were covered with a sheet of gel with BCDAT medium containing 50  $\mu$ g ml<sup>-1</sup> zeocin and 10  $\mu$ g ml<sup>-1</sup> PI. After 6h of observation, the gel was removed, and the gametophores were gently washed. The gametophores were then covered with solid BCDAT medium with 10  $\mu$ g ml<sup>-1</sup> PI without zeocin, and observation was resumed. Bright-field and PI fluorescence images of two or three leaves of each gametophore were obtained every 2h under a fluorescence microscope (IX81, Olympus).

**Comet assay.** A comet assay was performed as previously described<sup>20,34,35</sup> with some modifications. Intact gametophores were collected into a 2.0 ml tube and frozen in liquid nitrogen. The nuclei were isolated by slicing the frozen tissue with a razor blade and mixing it with 0.8% low-melting-temperature agarose (NuSieve GTG Agarose, cat. no. 50080) preheated to 42°C. The agarose containing the nuclei was spread onto an agarose-coated glass slide. After the agarose had solidified, the slide was immersed in lysing solution (2.5 M NaCl, 10 mM Tris-HCl (pH 7.6), 0.1 M EDTA and 1% N-lauroyl sarcosinate) for 1h at room temperature in the dark and rinsed in 1  $\times$  TBE buffer for 5 min. For the N/N comet assay, the slides were submerged in fresh neutral electrophoresis buffer (1  $\times$  TBE) and subjected to electrophoresis for 4 min at 20 V (0.8 V cm<sup>-1</sup>). For the A/A comet

assay, after lysing and washing with TBE buffer, the slides were submerged in unwinding solution (0.3 M NaOH, 5 mM EDTA and 1 M NaCl) for 20 min at room temperature to denature the DNA molecules. The slide was rinsed in alkaline rinse solution (0.04 M NaOH and 2 mM EDTA) for 2 min, submerged in fresh alkaline electrophoresis buffer (0.03 M NaOH and 2 mM EDTA) and subjected to electrophoresis for 4 min at 20 V (0.8 V cm<sup>-1</sup>). After electrophoresis, the slides were dehydrated in increasing concentrations of ethanol and air dried for at least 30 min. The DNA was stained with 1× SYBR Gold (Invitrogen) and observed under a fluorescence microscope (BX60, Olympus) equipped with a ×20 objective lens (Olympus), a filter cube (Olympus) and a digital charge-coupled device (CCD) camera (ORCA-R2, Hamamatsu Photonics). The DNA comet images were analysed using OpenComet, a plugin of Fiji v.1.0 for the automated analysis of DNA comet images<sup>36</sup>. The box plots were prepared with R v.3.5.1 (ref. <sup>37</sup>) using the `geom_boxplot` function in the `ggplot2` package<sup>38</sup>.

**Plasmid construction.** The primers used for plasmid construction are listed in Supplementary Table 1. To produce the deletion mutant of the kinase domain region of *ATM*, the middle and 3'-flanking regions were amplified and inserted into the *EcoRV* and *SmaI* sites of the pTN182 plasmid (AB267706), respectively (Supplementary Fig. 4a). To produce the deletion mutant of *ATR*, the 5'- and 3'-flanking regions were amplified by PCR and inserted into the *EcoRV* and *SmaI* sites of the pTN186 plasmid (AB542059), respectively (Supplementary Fig. 5a). The newly generated constructs were linearized with suitable restriction enzymes for gene targeting. The knockout mutants of *ATM* and *ATR* were generated using the CRISPR–Cas9 system<sup>25</sup>. The primers were designed using CRISPRdirect (<http://crispr.dncls.jp/>) to produce single-guide RNAs (sgRNAs) targeting *ATM* or *ATR*. The primers were dimerized and cloned into the *BsaI* site of the sgRNA expression plasmid pPpU6–sgRNA (LC494193). For *ATM*, two constructs, pPpU6–*ATM*–sgRNA#1 and pPpU6–*ATM*–sgRNA#2, were generated to target two different positions in *ATM* (Supplementary Fig. 4c). For *ATR*, three constructs, pPpU6–*ATR*–sgRNA#1, pPpU6–*ATR*–sgRNA#2 and pPpU6–*ATR*–sgRNA#3, were generated to target three different positions in *ATR* (Supplementary Figs. 5c and 7a).

**Transformation and selection of transformants.** All constructs were introduced into protoplasts by PEG-mediated transformation as described previously<sup>32</sup>. The stable deletion lines of *ATM* and *ATR* were screened by PCR and analysed by DNA gel blot analysis to confirm the single integration (Supplementary Figs. 4b and 5b). For CRISPR-mediated transformation, each pPpU6–sgRNA construct was cotransformed into protoplasts with pAct–Cas9 and pActHyR (ref. <sup>25</sup>). Indel mutations in *ATM* and *ATR* were analysed by sequencing the PCR products from the genomic region targeted by each sgRNA (Supplementary Figs. 4c, 5c and 7a).

**Removing the zeocin resistance cassette.** The zeocin resistance cassette p35S-loxP-zeo (AB540628) was introduced into the genome to produce *STEMIN2* (ref. <sup>2</sup>) or *CSP4* (ref. <sup>15</sup>) deletion lines. To analyse the phenotypes induced by zeocin treatment in these zeocin-resistant lines ( $\Delta$ csp1 $\Delta$ csp2 $\Delta$ csp3 $\Delta$ csp4 #29,  $\Delta$ stemin2 #29,  $\Delta$ stemin1 $\Delta$ stemin2 #33 and  $\Delta$ stemin1 $\Delta$ stemin2 $\Delta$ stemin3 #6–48)<sup>2,15</sup>, the zeocin resistance cassette had to be removed. Circular plasmid pTN75 (AB542060) containing the Cre recombinase<sup>39</sup> cassette was transiently expressed in these lines via PEG-mediated transformation. The Cre recombinase excised the zeocin resistance cassette, which was located between two loxP sites, from the genome. The newly generated lines were renamed  $\Delta$ csp1 $\Delta$ csp2 $\Delta$ csp3 $\Delta$ csp4 #29–1,  $\Delta$ stemin2 #29–1,  $\Delta$ stemin1 $\Delta$ stemin2 #33–1 and  $\Delta$ stemin1 $\Delta$ stemin2 $\Delta$ stemin3 #6–48–1, and the loss of zeocin resistance was confirmed on the basis of their failure to grow on a medium containing 50  $\mu$ g ml<sup>-1</sup> zeocin.

**Microscopy.** The images of excised leaves were captured under a fluorescence microscope (BX51, Olympus) equipped with a colour CCD camera (DS-Fi1c, Nikon) or under a fluorescence microscope (BX60, Olympus) equipped with a monochromatic CCD camera (ORCA-R2, Hamamatsu Photonics). The images of intact gametophores were captured under a fluorescence stereomicroscope (SZX16, Olympus) equipped with a colour CMOS camera (DP74, Olympus) or under a microscope (M205c, Leica) equipped with a colour CMOS camera (DMC5400, Leica). sGFP fluorescence was observed with a GFPHQ filter (Olympus) to reduce the autofluorescence from chloroplasts. The time-lapse imaging was performed under a fluorescence microscope (IX81, Olympus) equipped with an EM-CCD camera (ImagEM X2, Hamamatsu Photonics).

**Transcriptome analysis.** The intact gametophores were treated with or without 50  $\mu$ g ml<sup>-1</sup> zeocin for 6 h, washed with liquid BCDAT medium and incubated in liquid BCDAT medium without zeocin for 48 h. Fifty to one hundred gametophores were collected at 0, 6, 12 and 54 h after cultivation without zeocin and at 1, 3, 6, 9, 12, 18, 30 and 54 h during and after cultivation with zeocin (Fig. 2c). After cutting to remove the protonemata, rhizoids and leaves near the bottom of the stem, the gametophores were frozen in liquid nitrogen. Total RNA was extracted with an RNeasy Plant Mini Kit (Qiagen) with DNase I following the manufacturer's recommendations. The RNA-seq libraries were prepared using a TruSeq Stranded mRNA Library Prep Kit (Illumina) and sequenced on

the HiSeq1500 (Illumina) platform following the manufacturer's protocol. The single-end reads were trimmed with cutadapt v.1.16 (ref. <sup>40</sup>) and mapped to the *P. patens* v.3.3 transcriptome (Phytozome v.12.1) using kallisto v.0.43.1 (ref. <sup>41</sup>) with the 100-time bootstrap option. The mapping results were analysed using the sleuth v.0.30.0 package<sup>42</sup> with R v.3.5.1 (ref. <sup>37</sup>). Hierarchical clustering of the samples was performed on the basis of transcripts per million values (Supplementary Fig. 2). Non-parametric dimensional reduction scaling was performed to visualize the samples in a two-dimensional plane, and transitional trajectories were estimated using a minimum spanning tree of the samples<sup>43</sup> with built-in functions in vegan package v.2.5–2 (Fig. 4a).

**Quantitative PCR with reverse transcription analysis.** Approximately 60 gametophores were treated with or without zeocin (50  $\mu$ g ml<sup>-1</sup>) for 6 h. The basal parts of the gametophores containing protonemata and rhizoids were removed. The remaining parts of the gametophores were collected and frozen in liquid nitrogen. Total RNA was extracted using an RNeasy Plant Micro Kit (Qiagen) with the DNase I treatment following the manufacturer's recommendations. First-strand complementary DNA was synthesized using a ReverTra Ace qPCR RT Master Mix kit (TOYOBO). Quantitative PCR with reverse transcription (RT–qPCR) was performed using a QuantStudio 3 Real-Time PCR Instrument (Thermo Fisher Scientific) with a THUNDERBIRD SYBR qPCR Mix kit (TOYOBO). The primers used for RT–qPCR are listed in Supplementary Table 2. The results were analysed using the 2<sup>- $\Delta\Delta$ Ct</sup> method<sup>44</sup>. The quantification of each sample was performed in technical triplicates and two biological replicates.

**Reporting Summary.** Further information on research design is available in the Nature Research Reporting Summary linked to this article.

## Data availability

The sequence data can be found in Phytozome *P. patens* v.3.3 (ref. <sup>45</sup>) (OE-JGI, <http://phytozome.jgi.doe.gov/>) under the following accession numbers: *ATM* (Pp3c2\_23700), *ATR* (Pp3c6\_3460), *STEMIN1* (Pp3c1\_27440), *STEMIN2* (Pp3c14\_9940), *STEMIN3* (Pp3c10\_7030), *CSP1* (Pp3c5\_6070), *CSP2* (Pp3c6\_23240), *CSP3* (Pp3c5\_7920) and *CSP4* (Pp3c5\_7880). RNA-seq data were deposited into the DDBJ Sequence Read Archive (DRA) under accession number DRA008745.

Received: 16 August 2019; Accepted: 16 July 2020;

Published online: 17 August 2020

## References

- Yoshiyama, K. O., Sakaguchi, K. & Kimura, S. DNA damage response in plants: conserved and variable response compared to animals. *Biology* **2**, 1338–1356 (2013).
- Ishikawa, M. et al. *Physcomitrella* STEMIN transcription factor induces stem cell formation with epigenetic reprogramming. *Nat. Plants* **5**, 681–690 (2019).
- Ikeuchi, M., Ogawa, Y., Iwase, A. & Sugimoto, K. Plant regeneration: cellular origins and molecular mechanisms. *Development* **143**, 1442–1451 (2016).
- Pilkington, M. The regeneration of the stem apex. *New Phytol.* **28**, 37–53 (1929).
- Reinhardt, D., Frenz, M., Mandel, T. & Kuhlemeier, C. Microsurgical and laser ablation analysis of interactions between the zones and layers of the tomato shoot apical meristem. *Development* **130**, 4073–4083 (2003).
- Heyman, J. et al. ERF115 controls root quiescent center cell division and stem cell replenishment. *Science* **342**, 860–863 (2013).
- Sena, G., Wang, X., Liu, H. Y., Hofhuis, H. & Birnbaum, K. D. Organ regeneration does not require a functional stem cell niche in plants. *Nature* **457**, 1150–1153 (2009).
- Zhou, W. et al. A Jasmonate signaling network activates root stem cells and promotes regeneration. *Cell* **177**, 942–956 (2019).
- Fulcher, N. & Sablowski, R. Hypersensitivity to DNA damage in plant stem cell niches. *Proc. Natl Acad. Sci. USA* **106**, 20984–20988 (2009).
- Johnson, R. A. et al. SUPPRESSOR OF GAMMA RESPONSE 1 links DNA damage response to organ regeneration. *Plant Physiol.* **176**, 1665–1675 (2017).
- Steward, F. C., Mapes, M. O. & Mears, K. Growth and organized development of cultured cells. II. Organization in cultures grown from freely suspended cells. *Am. J. Bot.* **45**, 705–709 (1958).
- Kareem, A. et al. PLETHORA genes control regeneration by a two-step mechanism. *Curr. Biol.* **25**, 1017–1030 (2015).
- Ishikawa, M. et al. *Physcomitrella* cyclin-dependent kinase A links cell cycle reactivation to other cellular changes during reprogramming of leaf cells. *Plant Cell* **23**, 2924–2938 (2011).
- Sato, Y. et al. Cells reprogramming to stem cells inhibit the reprogramming of adjacent cells in the moss *Physcomitrella patens*. *Sci. Rep.* **7**, 1909 (2017).
- Li, C. et al. A Lin28 homolog reprograms differentiated cells to stem cells in the moss *Physcomitrella patens*. *Nat. Commun.* **8**, 14242 (2017).
- Kofuji, R. & Hasebe, M. Eight types of stem cells in the life cycle of the moss *Physcomitrella patens*. *Curr. Opin. Plant Biol.* **17**, 13–21 (2014).

17. Chankova, S. G., Dimova, E., Dimitrova, M. & Bryant, P. E. Induction of DNA double-strand breaks by zeocin in *Chlamydomonas reinhardtii* and the role of increased DNA double-strand breaks rejoining in the formation of an adaptive response. *Radiat. Environ. Biophys.* **46**, 409–416 (2007).
18. Chen, J., Ghorai, M. K., Kenney, G. & Stubbe, J. A. Mechanistic studies on bleomycin-mediated DNA damage: multiple binding modes can result in double-stranded DNA cleavage. *Nucleic Acids Res.* **36**, 3781–3790 (2008).
19. Sakasai, R. & Iwabuchi, K. The distinctive cellular responses to DNA strand breaks caused by a DNA topoisomerase I poison in conjunction with DNA replication and RNA transcription. *Genes Genet. Syst.* **90**, 187–194 (2015).
20. Angelis, K. J., Dušinská, M. & Collins, A. R. Single cell gel electrophoresis: detection of DNA damage at different levels of sensitivity. *Electrophoresis* **20**, 2133–2138 (1999).
21. Lanier, C., Manier, N., Cuny, D. & Deram, A. The comet assay in higher terrestrial plant model: review and evolutionary trends. *Environ. Pollut.* **207**, 6–20 (2015).
22. Jones, K., Kim, D. W., Park, J. S. & Khang, C. H. Live-cell fluorescence imaging to investigate the dynamics of plant cell death during infection by the rice blast fungus *Magnaporthe oryzae*. *BMC Plant Biol.* **16**, 69 (2016).
23. Antosiewicz-Bourget, J. et al. Induced pluripotent stem cell lines derived from human somatic cells. *Science* **318**, 1917–1920 (2007).
24. Hu, Z., Cools, T. & De Veylder, L. Mechanisms used by plants to cope with DNA damage. *Annu. Rev. Plant Biol.* **67**, 439–462 (2016).
25. Collonnier, C. et al. CRISPR–Cas9-mediated efficient directed mutagenesis and RAD51-dependent and RAD51-independent gene targeting in the moss *Physcomitrella patens*. *Plant Biotechnol. J.* **15**, 122–131 (2017).
26. Hong, J. H. et al. A sacrifice-for-survival mechanism protects root stem cell niche from chilling stress. *Cell* **170**, 102–113 (2017).
27. Sharma, P., Jha, A. B., Dubey, R. S. & Pessarakli, M. Reactive oxygen species, oxidative damage, and antioxidative defense mechanism in plants under stressful conditions. *J. Bot.* **2012**, 217037 (2012).
28. Rodriguez, E., Azevedo, R., Fernandes, P. & Santos, C. Cr(VI) induces DNA damage, cell cycle arrest and polyploidization: a flow cytometric and comet assay study in *Pisum sativum*. *Chem. Res. Toxicol.* **24**, 1040–1047 (2011).
29. Gehring, M., Reik, W. & Henikoff, S. DNA demethylation by DNA repair. *Trends Genet.* **25**, 82–90 (2009).
30. Gursoy-Yuzugullu, O., House, N. & Price, B. D. Patching broken DNA: nucleosome dynamics and the repair of DNA breaks. *J. Mol. Biol.* **428**, 1846–1860 (2016).
31. Rensing, S. A. et al. The *Physcomitrella* genome reveals evolutionary insights into the conquest of land by plants. *Science* **319**, 64–69 (2008).
32. Nishiyama, T., Hiwatashi, Y., Sakakibara, K., Kato, M. & Hasebe, M. Tagged mutagenesis and gene-trap in the moss, *Physcomitrella patens* by shuttle mutagenesis. *DNA Res.* **7**, 9–17 (2000).
33. Aoyama, T. et al. AP2-type transcription factors determine stem cell identity in the moss *Physcomitrella patens*. *Development* **139**, 3120–3129 (2012).
34. Enciso, M., Sarasa, J., Agarwal, A., Fernández, J. L. & Gosálvez, J. A two-tailed comet assay for assessing DNA damage in spermatozoa. *Reprod. Biomed. Online* **18**, 609–616 (2009).
35. Cortés-Gutiérrez, E. I., Fernández, J. L., Dávila-Rodríguez, M. I., López-Fernández, C. & Gosálvez, J. Two-tailed comet assay (2T-Comet): simultaneous detection of DNA single and double strand breaks. *Methods Mol. Biol.* **1560**, 285–293 (2017).
36. Gyori, B. M., Venkatachalam, G., Thiagarajan, P. S., Hsu, D. & Clement, M. V. OpenComet: an automated tool for comet assay image analysis. *Redox Biol.* **2**, 457–465 (2014).
37. R: A Language and Environment for Statistical Computing v.3.5.1 (R Core Team, 2018); <https://doi.org/10.1787/csp-aut-table-2018-1-en>
38. Wickham, H. ggplot2: Elegant graphics for data analysis v.3.2.1 [https://doi.org/10.1007/978-3-319-24277-4\\_2](https://doi.org/10.1007/978-3-319-24277-4_2) (2016).
39. Odell, J., Caimi, P., Sauer, B. & Russell, S. Site-directed recombination in the genome of transgenic tobacco. *Mol. Gen. Genet.* **223**, 369–378 (1990).
40. Martin, M. Cutadapt removes adapter sequences from high-throughput sequencing reads. *EMBnet J.* **17**, 10–12 (2011).
41. Bray, N. L., Pimentel, H., Melsted, P. & Pachter, L. Near-optimal probabilistic RNA-seq quantification. *Nat. Biotechnol.* **34**, 525–527 (2016).
42. Pimentel, H., Bray, N. L., Puente, S., Melsted, P. & Pachter, L. Differential analysis of RNA-seq incorporating quantification uncertainty. *Nat. Methods* **14**, 687–690 (2017).
43. Jari, O. et al. vegan: Community ecology package. R package v.2.5-2 (2018).
44. Livak, K. J. & Schmittgen, T. D. Analysis of relative gene expression data using real-time quantitative PCR and the 2<sup>-ΔΔCT</sup> method. *Methods* **25**, 402–408 (2001).
45. Lang, D. et al. The *Physcomitrella patens* chromosome-scale assembly reveals moss genome structure and evolution. *Plant J.* **93**, 515–533 (2018).

## Acknowledgements

We thank F. Nogué for providing the CRISPR–Cas9-related vectors; Y. Horiuchi for modifying the sgRNA expression vector; S. Ooi, E. Aoki, M. Goto, T. Nishi, I. Kajikawa and T. Masuoka for technical assistance; and B. Scheres for comments on the draft. The moss cultivation and RNA-seq were supported in part by the Model Plant Research Facility, Functional Genomics Facility, and Data Integration and Analysis Facility at the National Institute for Basic Biology, Japan. N.G. was supported by the RA program of the National Institute for Basic Biology, a scholarship from the China Scholarship Council (no. 201506760024) and a “Double World-classes” development scholarship from Huazhong Agricultural University, the College of Life Science and Technology. This work was partially supported by JSPS KAKENHI grant nos. JP16K14760, JP18H04790 and JP19H05274 to Y.T., 18H04846 to M.I., and 16H06378 to Y.T., M.I. and M.H.; the Young Researcher Overseas Visits Program for Vitalizing Brain Circulation to A.I., M.I., Y.T. and M.H.; the NIBB Collaborative Research Program (grant nos. 18-345 and 19-313), the National Natural Science Foundation of China (grant no. 31672112), Fundamental Research Funds for the Central Universities in China (grant no. 2662018PY099) and the Advanced Foreign Experts Project (grant no. G20190017014) to C.C.; and the Ministry of Education, Youth, and Sports of the Czech Republic grant no. LTC17047/2017 to K.J.A.

## Author contributions

N.G., Y.T., A.I., C.C. and M.H. conceived and designed the research. N.G. and Y.T. performed the experiments. S.S. performed the mRNA sequencing. G.P. analysed the RNA-seq data. Y.K. performed the transformations. A.I. and K.J.A. contributed to the comet assay. M.I. provided mutant lines of *STEMINS*. N.G. prepared the figures. N.G. and Y.T. wrote the manuscript with contributions from M.I., C.C. and M.H.

## Competing interests

The authors declare no competing interests.

## Additional information

**Extended data** is available for this paper at <https://doi.org/10.1038/s41477-020-0745-9>.

**Supplementary information** is available for this paper at <https://doi.org/10.1038/s41477-020-0745-9>.

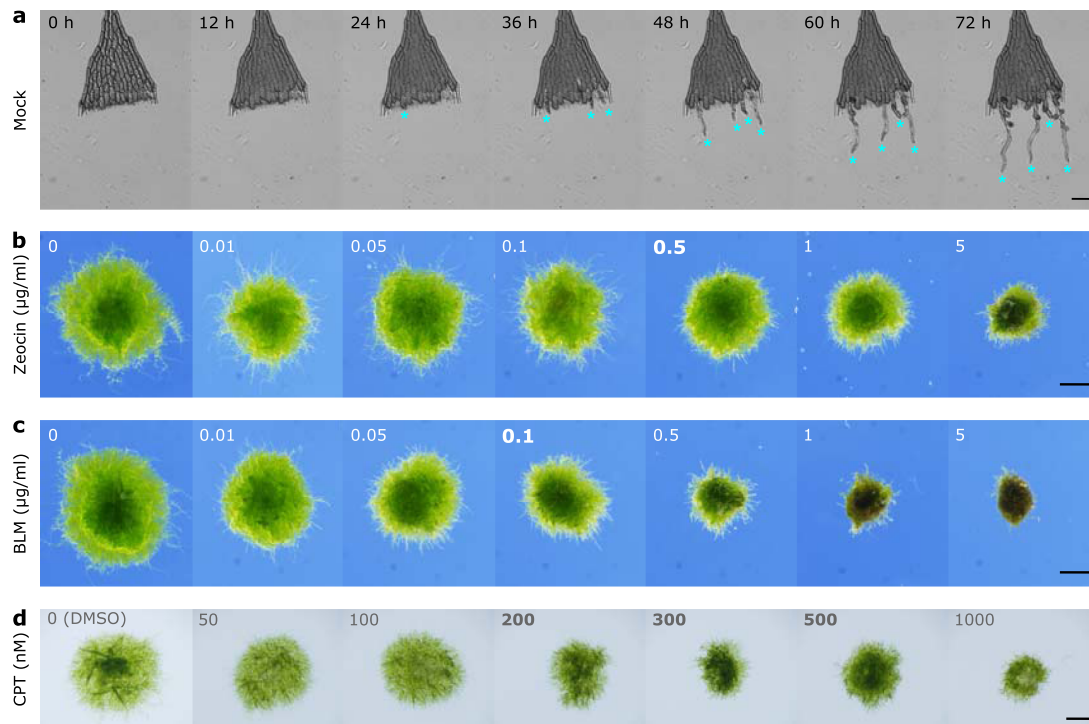
**Correspondence and requests for materials** should be addressed to C.C. or M.H.

**Peer review information** *Nature Plants* thanks Anne Britt, Robert Sablowski and the other, anonymous, reviewer(s) for their contribution to the peer review of this work.

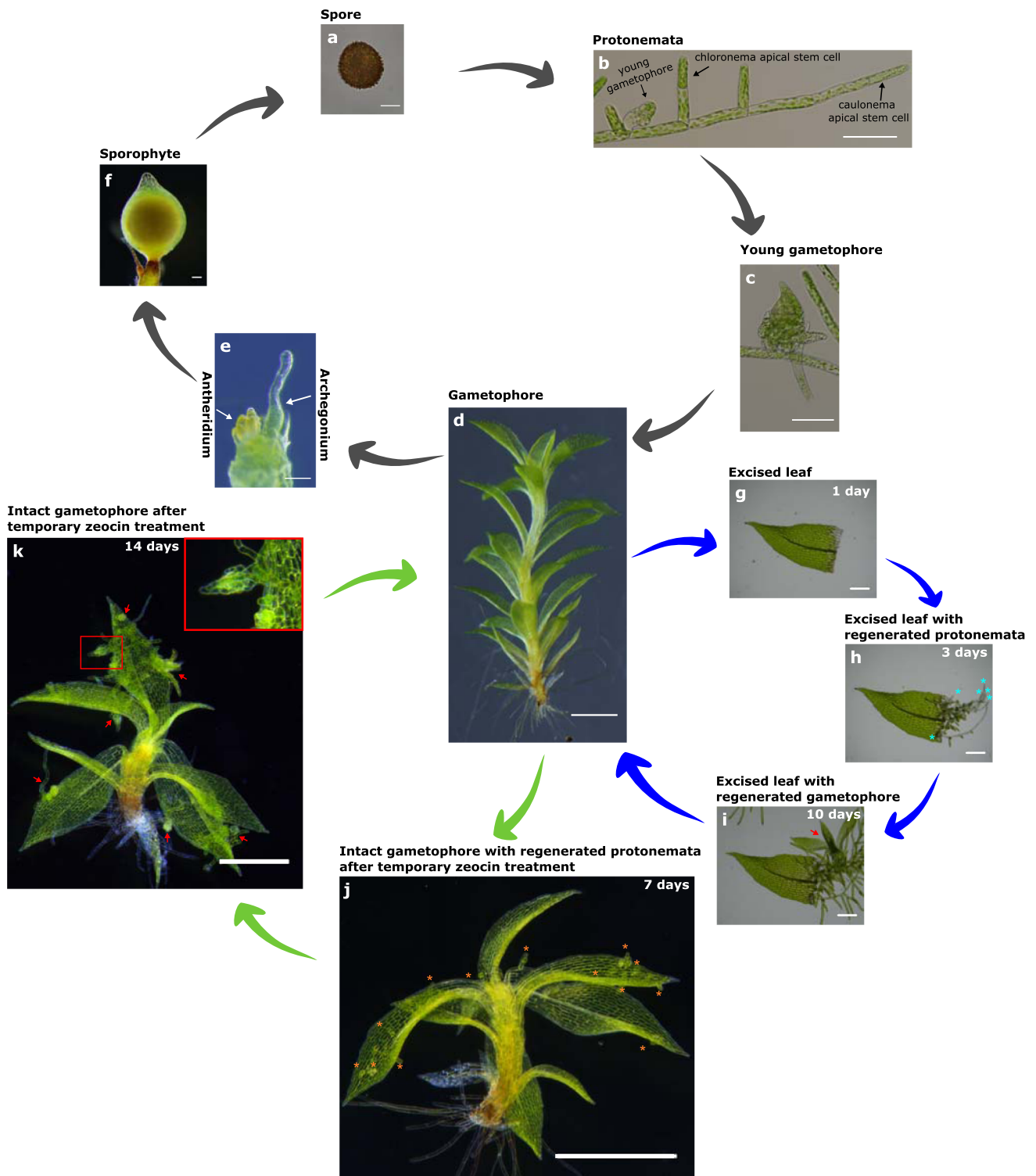
**Reprints and permissions information** is available at [www.nature.com/reprints](http://www.nature.com/reprints).

**Publisher's note** Springer Nature remains neutral with regard to jurisdictional claims in published maps and institutional affiliations.

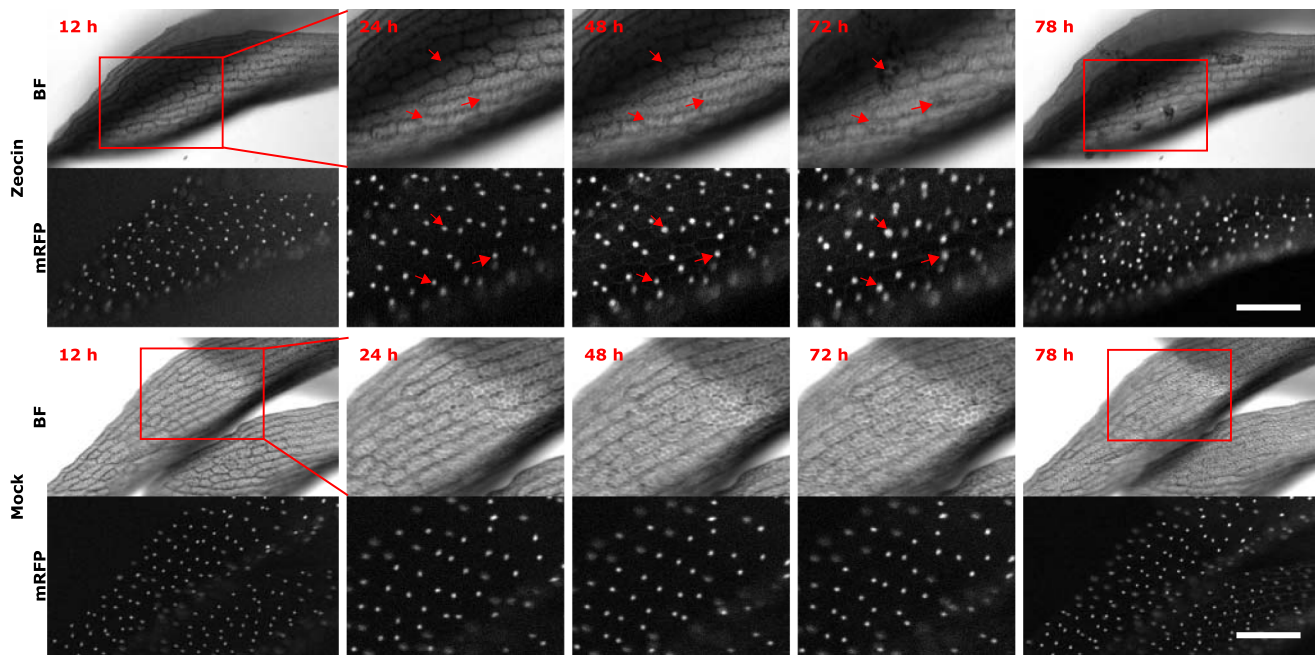
© The Author(s), under exclusive licence to Springer Nature Limited 2020



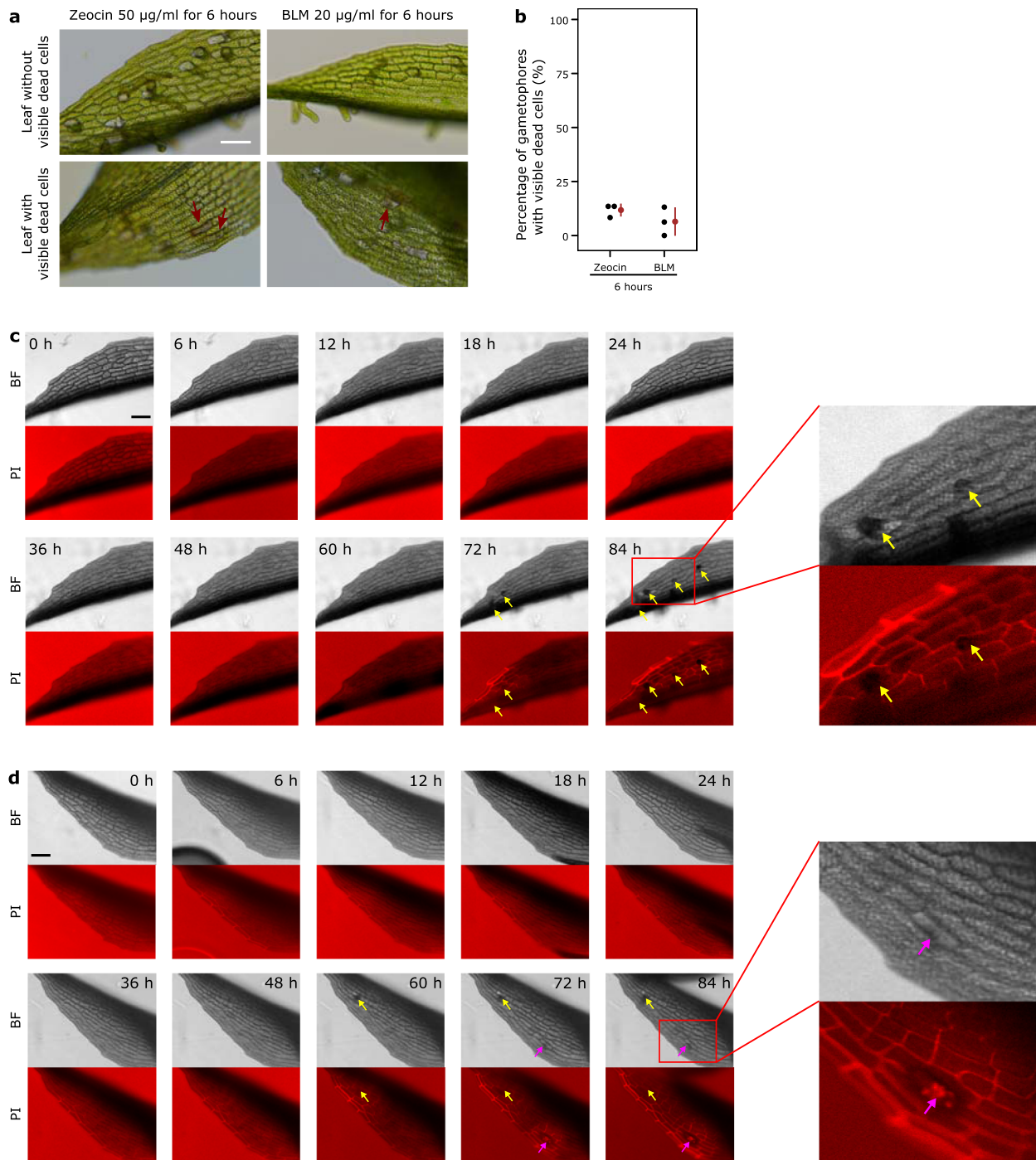
**Extended Data Fig. 1 | DNA strand break-inducing reagents attenuate the growth of protonemata.** **a** A representative wild-type leaf at 0, 12, 24, 36, 48, 60, and 72 hours after excision. Blue asterisks indicate the positions of chloronema apical stem cells generated from the edge cells of the excised leaf. The reprogramming of excised leaves was observed in more than two independent experiments with similar results. **b–d** Representative one-week-old wild-type plants on solid BCDAT medium with or without various concentrations of zeocin (**b**), bleomycin (BLM) (**c**), or camptothecin (CPT) (**d**). Protonema growth slowed under the treatment with 0.5  $\mu\text{g/ml}$  zeocin, 0.1  $\mu\text{g/ml}$  BLM, or 200 nM CPT. Three plants in each concentration of zeocin, BLM, or CPT were observed twice independently with similar results. Scale bars: 100  $\mu\text{m}$  in (**a**), 1 mm in (**b–d**).



**Extended Data Fig. 2 | Newly formed gametophores in protonemata regenerated from intact gametophore leaves after zeocin treatment.** **a–f** Top panels connected by gray arrows show the life cycle of *Physcomitrella*. A representative image at each developmental stage is shown. **d, g–i** Right-bottom panels connected by blue arrows show the regeneration process of excised leaves. Red arrow in **(i)** indicates a young gametophore formed from protonemata (essentially the same as shown in **[b]**), which were generated from excised leaves. These new gametophores frequently developed near the original excised leaf. **d, j** and **k** Left-bottom panels connected by green arrows show the regeneration process from intact gametophores after temporary zeocin treatment. Wild-type intact gametophores were treated with 50  $\mu\text{g/ml}$  zeocin for 6 hours and incubated in BCDAT liquid medium without a DNA damage reagent for an additional 2 weeks. Orange asterisks in **(j)** indicate the positions of chloronema apical stem cells generated from differentiated gametophore leaf cells. Red arrows in **(k)** indicate young gametophores formed from protonemata (essentially the same as shown in **[b]**) generated from leaves. These newly formed gametophores developed near the leaf. The growth of protonemata cells was attenuated in liquid medium. Similar results were obtained using 20 to 25 gametophores in three independent experiments. Scale bars: 20  $\mu\text{m}$  in **(a)**; 100  $\mu\text{m}$  in **(b, c, e, f)**; 1 mm in **(d, j, k)**; 200  $\mu\text{m}$  in **(g–i)**.

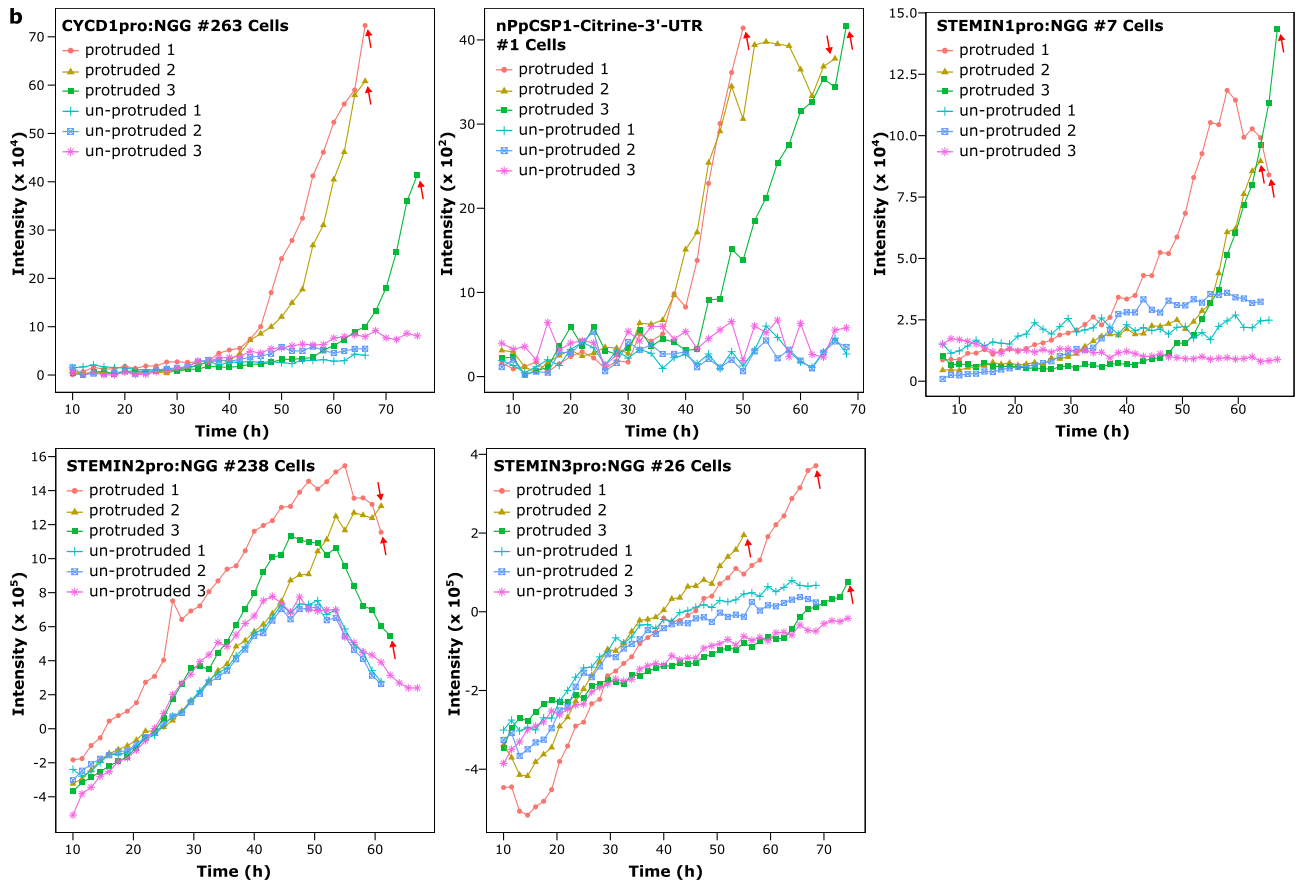
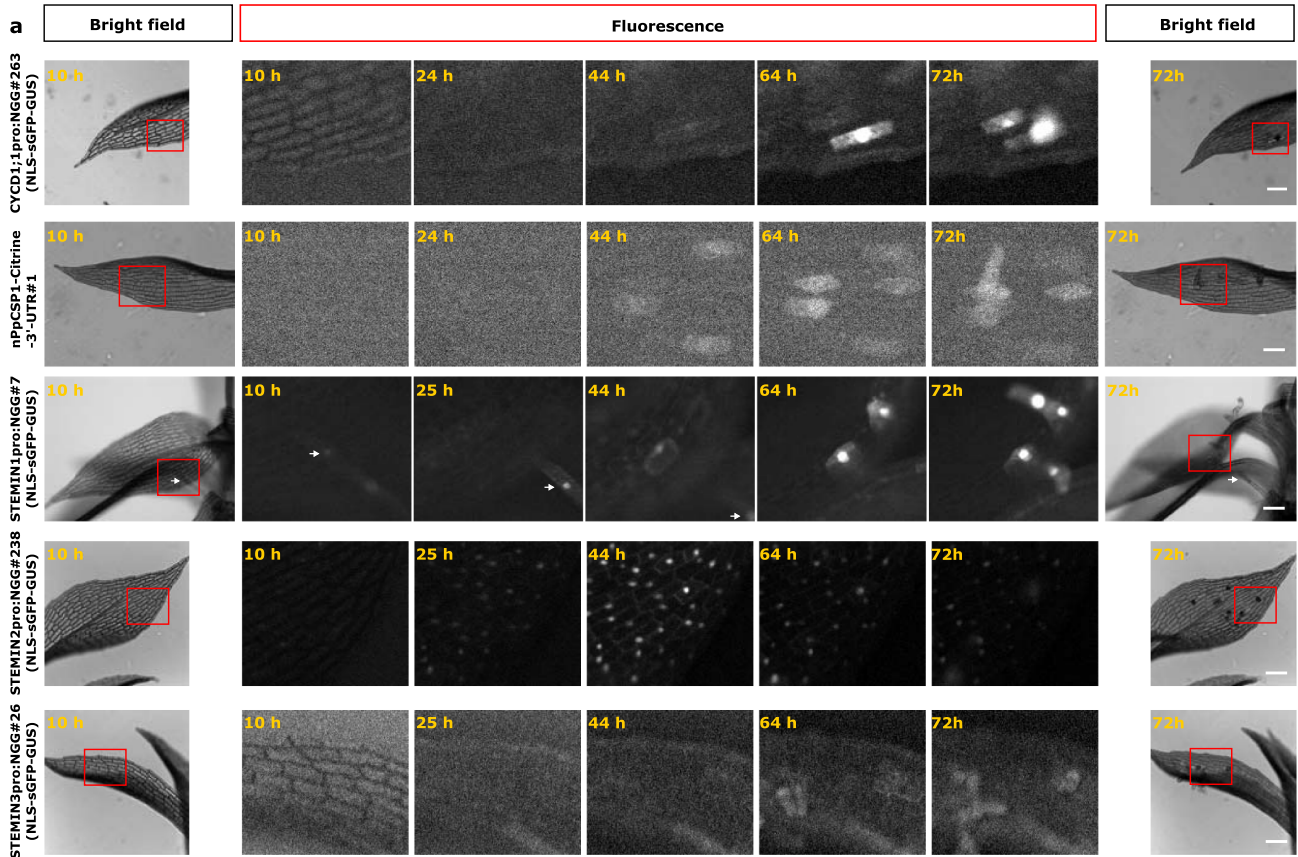


**Extended Data Fig. 3 | Protrusion of chloronema apical stem cells from leaf cells after temporary zeocin treatment.** Representative leaf of an intact gametophore of the H2B-mRFP<sup>14</sup> line, with nuclei labeled with histone H2B-mRFP fusion proteins, after 6 hours of 50  $\mu\text{g}/\text{ml}$  zeocin (top panels) or mock (bottom panels) treatment. Bright-field (BF) and fluorescence images (mRFP) were collected at 2-hour intervals; images taken at 12, 24, 48, 72, and 78 hours after the initiation of treatment are shown. Images taken at 24, 48, and 72 hours are 1.75 $\times$  magnified views of the regions highlighted by red squares in the images taken at 12 and 78 hours. Red arrows indicate leaf cells that were ultimately reprogrammed into chloronema stem cells. The experiments were performed twice independently with similar results. Scale bars: 200  $\mu\text{m}$ .



Extended Data Fig. 4 | See next page for caption.

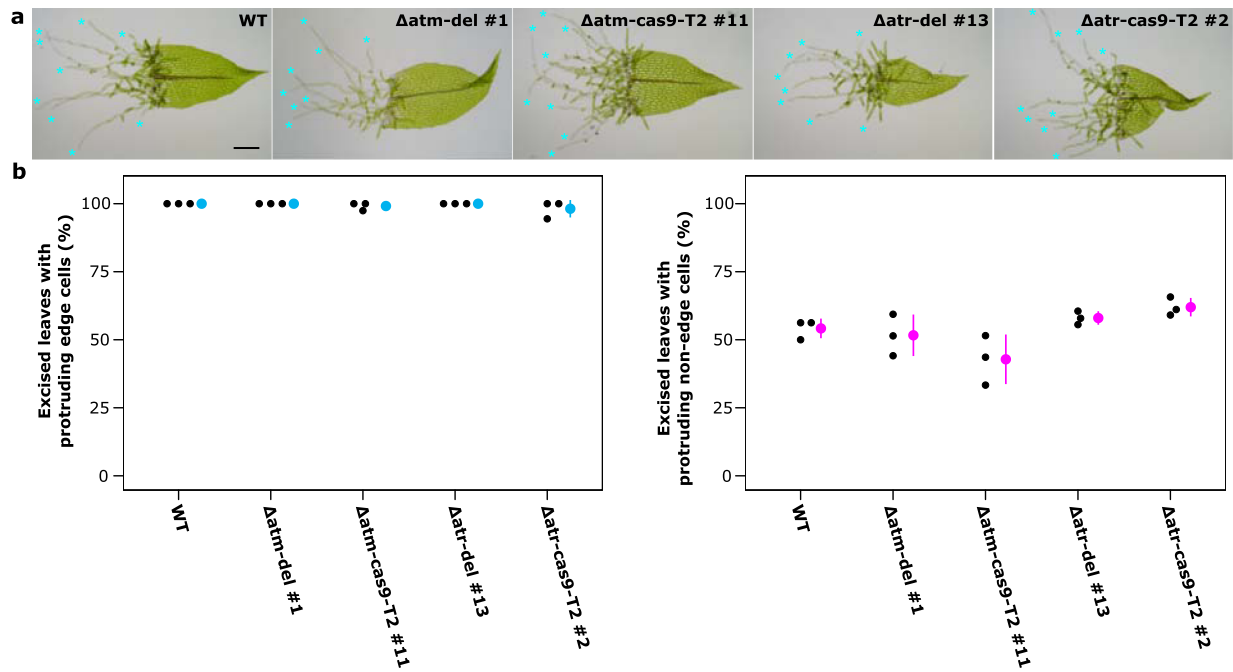
**Extended Data Fig. 4 | Reprogramming induced by transient zeocin treatment occurs independently of dead cells.** **a** Representative leaves without (top panels) or with visible dead cells (bottom panels) after transient zeocin or BLM treatment for 6 hours, followed by 7 days of cultivation without DNA damage reagents. Red arrows indicate dead cells in brown. **b** Percentage of gametophores with at least one visible dead leaf cell. Dark red dots and bars represent the mean and SD from three independent experiments ( $30 \leq n \leq 42$ , gametophores), respectively. **c** Bright-field (BF) and PI fluorescence images (PI) of a representative gametophore leaf without dead cells during and after 50  $\mu\text{g}/\text{ml}$  zeocin treatment for 6 hours. Images taken at 0, 6 (just before washing out zeocin), 12, 24, 36, 48, 60, 72, and 84 h from the time-lapse images (Supplementary Video 1) are shown. Yellow arrows indicate reprogrammed cells with protrusion. Although PI does not penetrate into apoplastic space of intact gametophore tissue, staining of cell wall with PI became visible after 64 h (Supplementary Video 1). After protrusion started in reprogrammed cells, PI fluorescence in cell walls of surrounding cells became visible, likely because of higher penetration in reprogrammed cells with tip growth. Similar results have been observed in 6 different gametophores. Since only the intercellular space of surrounding cells were stained by PI and none of the cells show nucleus staining, no imperceptible dead cells existed around the protruding reprogrammed cells to trigger the reprogramming. **d** Bright-field (BF) and PI fluorescence images (PI) of a representative gametophore leaf with dead cells during and after 50  $\mu\text{g}/\text{ml}$  zeocin treatment for 6 hours. Images were taken from the time-lapse images (Supplementary Video 2) at the same timepoints as those in **(c)**. Yellow and pink arrows indicate reprogrammed cells with protrusion and dead cells, respectively. After protrusion started in reprogrammed cells, PI fluorescence in cell walls of surrounding cells became visible, likely because of higher penetration in reprogrammed cells with tip growth. Also, PI fluorescence was detected in cell walls surrounding dead cells. Similar results have been observed in 2 different gametophores. Scale bars: 100  $\mu\text{m}$  in **(a)**; 100  $\mu\text{m}$  in **(c, d)**.



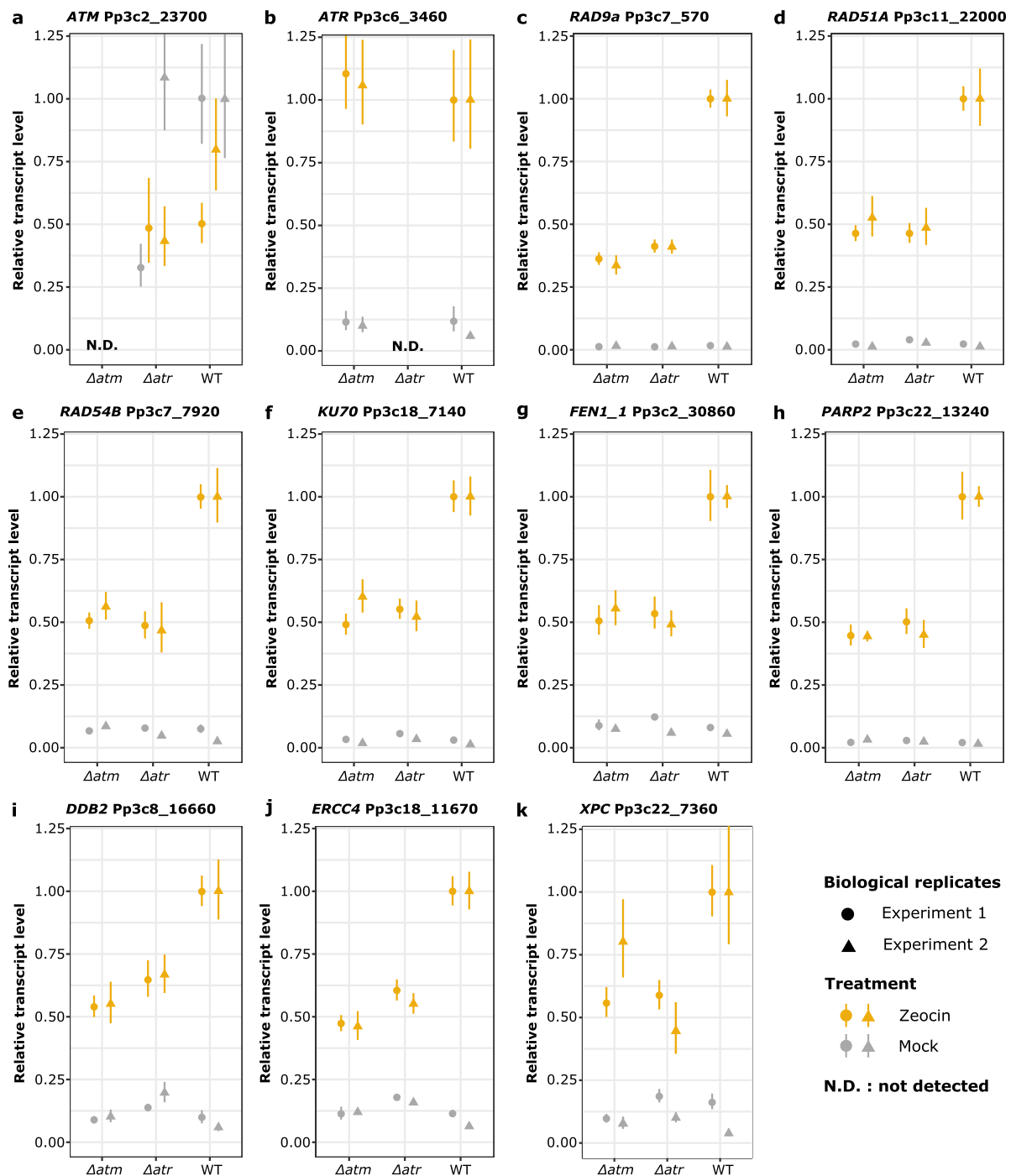
Extended Data Fig. 5 | See next page for caption.

**Extended Data Fig. 5 | Induction of *CYCD1;1*, *CSP1*, *STEMIN1*, and closely related genes in reprogramming cells after transient zeocin treatment. **a****

Representative gametophore leaves of *CYCD1;1*pro:NGG (NLS-sGFP-GUS) #263<sup>13</sup>, nPpCSP1-Citrine-3'UTR #1<sup>15</sup>, *STEMIN1*pro:NGG #7, *STEMIN2*pro:NGG #238, and *STEMIN3*pro:NGG #26<sup>2</sup> after 6 hours of 50 µg/ml zeocin treatment. Bright-field images taken at 10 and 72 h and fluorescent images taken at 10, 24, or 25, 44, 64, and 72 h from time-lapse images (Supplementary Videos 3-7) are shown. White arrows in the middle panels indicate chloronema cells near the observed leaf. The experiments were performed twice independently with similar results. Scale bars: 200 µm. **b** Intensities of sGFP or Citrine signals in three independent protruded and un-protruded cells of intact gametophore leaves of the lines described in **(a)** after zeocin treatment. Signal intensity was measured with Fiji 1.0. Red arrows indicate time points at which the cells began to protrude.



**Extended Data Fig. 6 | Neither *ATM* nor *ATR* deletions affect reprogramming induced by wounding. **a**** Representative wild-type,  $\Delta atm$ , and  $\Delta atr$  leaves cultured for 3 days after excision. **b** Percentages of wild-type,  $\Delta atm$ , and  $\Delta atr$  leaves with protruding edge cells (left) and non-edge cells (right) cultured for 3 days after excision. Blue and violet dots and bars represent the mean and SD from three independent experiments ( $n = 32$ , excised leaves), respectively. Scale bar: 200  $\mu m$  in (**a**).



**Extended Data Fig. 7 | Transcript levels of DNA damage response genes with or without zeocin treatment in  $\Delta atm$  or  $\Delta atr$  deletion mutants. a–k** Relative transcript levels of the genes in  $\Delta atm$ -del #1,  $\Delta atr$ -del #13, and wild type with (orange dots and lines) or without zeocin treatment (gray dots and lines) for 6 hours detected with RT-qPCR. Primers used in RT-qPCR are shown in Supplementary Table 2. The highest transcript value of each gene was normalized to 1.0. Dots and bars indicate means and SD of the technical triplicates ( $n = 3$ ). Two biological replicates were analyzed with similar result.

## Reporting Summary

Nature Research wishes to improve the reproducibility of the work that we publish. This form provides structure for consistency and transparency in reporting. For further information on Nature Research policies, see [Authors & Referees](#) and the [Editorial Policy Checklist](#).

### Statistics

For all statistical analyses, confirm that the following items are present in the figure legend, table legend, main text, or Methods section.

n/a Confirmed

- The exact sample size ( $n$ ) for each experimental group/condition, given as a discrete number and unit of measurement
- A statement on whether measurements were taken from distinct samples or whether the same sample was measured repeatedly
- The statistical test(s) used AND whether they are one- or two-sided  
*Only common tests should be described solely by name; describe more complex techniques in the Methods section.*
- A description of all covariates tested
- A description of any assumptions or corrections, such as tests of normality and adjustment for multiple comparisons
- A full description of the statistical parameters including central tendency (e.g. means) or other basic estimates (e.g. regression coefficient) AND variation (e.g. standard deviation) or associated estimates of uncertainty (e.g. confidence intervals)
- For null hypothesis testing, the test statistic (e.g.  $F$ ,  $t$ ,  $r$ ) with confidence intervals, effect sizes, degrees of freedom and  $P$  value noted  
*Give  $P$  values as exact values whenever suitable.*
- For Bayesian analysis, information on the choice of priors and Markov chain Monte Carlo settings
- For hierarchical and complex designs, identification of the appropriate level for tests and full reporting of outcomes
- Estimates of effect sizes (e.g. Cohen's  $d$ , Pearson's  $r$ ), indicating how they were calculated

*Our web collection on [statistics for biologists](#) contains articles on many of the points above.*

### Software and code

Policy information about [availability of computer code](#)

Data collection

RNA-seq: HiSeq1500 (Illumina)  
qRT-PCT: QuantStudio® 3 Real-Time PCR Instrument (Thermo Fisher Scientific)

Data analysis

Comet assay and Microscopy: "OpenComet" version 1.3.1 (<http://www.cometbio.org>); Fiji version 1.0  
RNA-seq and qRT-PCR: Cutadapt version 1.16; Kallisto version 0.43.1; Sleuth version 0.30.0; R version 3.5.1; Vegan package 2.5-2; ggplot2 package 3.2.1

For manuscripts utilizing custom algorithms or software that are central to the research but not yet described in published literature, software must be made available to editors/reviewers. We strongly encourage code deposition in a community repository (e.g. GitHub). See the Nature Research [guidelines for submitting code & software](#) for further information.

### Data

Policy information about [availability of data](#)

All manuscripts must include a [data availability statement](#). This statement should provide the following information, where applicable:

- Accession codes, unique identifiers, or web links for publicly available datasets
- A list of figures that have associated raw data
- A description of any restrictions on data availability

Sequence data can be found in Phytozome P. patens V3.3 (OE-JGI, <http://phytozome.jgi.doe.gov/>) under the following accession numbers: ATM (Pp3c2\_23700); ATR (Pp3c6\_3460); STEMIN1 (Pp3c1\_27440); STEMIN2 (Pp3c14\_9940); STEMIN3 (Pp3c10\_7030); CSP1 (Pp3c5\_6070); CSP2 (Pp3c6\_23240); CSP3 (Pp3c5\_7920); and CSP4 (Pp3c5\_7880). RNA-seq data were deposited into DDBJ Sequence Read Archive (DRA) under accession number DRA008745.

## Field-specific reporting

Please select the one below that is the best fit for your research. If you are not sure, read the appropriate sections before making your selection.

Life sciences       Behavioural & social sciences       Ecological, evolutionary & environmental sciences

For a reference copy of the document with all sections, see [nature.com/documents/nr-reporting-summary-flat.pdf](https://www.nature.com/documents/nr-reporting-summary-flat.pdf)

## Life sciences study design

All studies must disclose on these points even when the disclosure is negative.

Sample size	Sample size of excised leaves and intact gametophores was selected based on our prior knowledge and experience (Ishikawa et al., 2011 Plant Cell 23, 2924-938; Sakakibara et al., 2014 Development 141, 1660-1670; Li et al., 2017 Nat. Commun. 8, 1-13) with at least three independent biological replicates. Sample size of comet assay was determined based on prior reported experience (Angelis, et al., 1999 Electrophoresis 20, 2133-2138; Lanier et al., 2015, Environ. Pollut. 207, 6-20). Comet assay was performed at least two independent biological replicates with similar results. In quantitative RT-PCR analysis, the quantification of each sample was performed in technical triplicates and two biological replicates. RNA-seq analysis was performed in three biological replicates.
Data exclusions	No data was excluded from all experiments.
Replication	We conducted all experiments with at least two biological replications using different biological samples. All replication experiments were successful.
Randomization	Plants were grown in growth chambers and gametophores were arbitrary randomly chosen and used for experiments. The comets were arbitrary randomly collected from each gel in the comet assay.
Blinding	To analyze the reprogramming rate of Physcomitrella gametophores after the DNA damage reagent treatment, the plants were cultured in growth chambers and their growth and experimental conditions were consistent. The assessment of the reprogramming phenotype after DNA damage reagent treatment depends on the clear morphologic maker, the protrusion of reprogrammed cells, under microscopic observation. So these experiments are not affected by the behavior of the investigators. The comet assay results were analyzed automatically using software, not manually. So blinding was not relevant to our study.

## Reporting for specific materials, systems and methods

We require information from authors about some types of materials, experimental systems and methods used in many studies. Here, indicate whether each material, system or method listed is relevant to your study. If you are not sure if a list item applies to your research, read the appropriate section before selecting a response.

### Materials & experimental systems

n/a	Involved in the study
<input checked="" type="checkbox"/>	<input type="checkbox"/> Antibodies
<input checked="" type="checkbox"/>	<input type="checkbox"/> Eukaryotic cell lines
<input checked="" type="checkbox"/>	<input type="checkbox"/> Palaeontology
<input checked="" type="checkbox"/>	<input type="checkbox"/> Animals and other organisms
<input checked="" type="checkbox"/>	<input type="checkbox"/> Human research participants
<input checked="" type="checkbox"/>	<input type="checkbox"/> Clinical data

### Methods

n/a	Involved in the study
<input checked="" type="checkbox"/>	<input type="checkbox"/> ChIP-seq
<input checked="" type="checkbox"/>	<input type="checkbox"/> Flow cytometry
<input checked="" type="checkbox"/>	<input type="checkbox"/> MRI-based neuroimaging